Wang, X.S., Sun, M., Cai, K.D., Zhao, G.C., Xiao, W.J., Xia, X.P., and Li, P.F., 2023, Crustal recycling and growth via mélange diapir in subduction zones: Insights from two episodes of magmatism in the Northern Yili Block, NW China: GSA Bulletin, https://doi.org/10.1130/B36447.1.

Supplemental Material

Supplementa1 Text S1. Analytical methods**.**

Figure S1. REE patterns of analyzed zircon from the granitoids in Northern Yili Block.

Figure S2. (a) SiO_2 vs $(^{87}Sr/_{86}Sr)_i$; (b) SiO_2 vs$(^{143}Nd/^{144}Nd)_i$ and (c) $^{147}Sm/^{144}Nd$ vs $(^{143}Nd/^{144}Nd)_i$ diagrams for granitoids of the Northern Yili Block.

Figure S3. Variation diagrams for major oxides versus SiO_2 for the magmatic rocks in the Northern Yili Block.

Table S1. Summary of zircon Lu–Hf and whole-rock Sr-Nd isotope data for the magmatic rocks from the Northern Yili block.

Table S2. LA-ICPMS zircon U-Pb isotopic analyses for the granitoid rocks from the Northern Yili Block.

Table S3. Zircon trace elemental contents of the magmatic rocks from the Northern Yili Block.

Table S4. Representative electron probe analyses of plagioclase and amphibole from the Kexiaxi dioritic microgranular enclaves and granodiorites.

Table S5. Major (wt.%) and trace element (ppm) data for the magmatic rocks from the Northern Yili Block.

Table S6. Zircon Lu-Hf isotopic compositions for the magmatic rocks from the Northern Yili Block.

Table S7. Whole Sr-Nd isotopic compositions of the granitoids from the Northern Yili Block.

Table S8. Nd-Hf isotopic compositions of the magmatic rocks from the Northern Yili Block.

Table S9. Compilations of the Whole-rock geochemical and isotopic compositions of the volcanic rocks from the Northern Yili Block.

SUPPLEMENTAL TEXT S1. ANALYTICAL METHODS

Zircon U-Pb dating

After sample crushing, zircon grains were separated by conventional heavy liquid and magnetic separation techniques. Zircon grains from the >25 μm non-magnetic fraction were hand-picked and mounted on adhesive tape, then enclosed in epoxy resin and polished to about half of their thickness. In order to investigate internal structures of potential analyzed zircons and choose potential target sites for U-Pb and Hf analyses, Cathodoluminescence (CL) images were obtained for zircons prior to analysis, using a JXA-8100 Electron Probe Micro-analyzer with a Mono CL3 Cathodoluminescence System for high resolution imaging and spectroscopy at Guangzhou Institute of Geochemistry, Chinese Academy of Sciences (GIG CAS).

In situ zircon U-Pb dating were measured at the Nanjing FocuMS Technology Co. Ltd. (FMS) by applying an Analyte Excite 193 nm ArF excimer laser ablation system attached to an Agilent Technologies 7700x quadrupole inductively couple plasma mass spectrometry system. The adopted working parameters are as follows: 8 Hz laser repetition rate, 6.0 J/cm^2 energy, and 40 μm spot diameter. Zircon standard 91500 (Wiedenbeck et al., 1995) was used for isotopic ratio correction, and zircon standard GJ-1 (Jackson et al., 2004) was analyzed as an unknown, after every eight sample measurements. A weighted mean $^{206}Pb/^{238}U$ age of 602±2 Ma (n = 40) was obtained for the latter, consistent, within error, with recommended age of 604±4 Ma (Jackson et al., 2004). Raw data were processed using ICPMSDataCal (Liu et al., 2010). Data reduction was carried out using the Isoplot/Ex 4.15 software (Ludwig, 2012). Zircon U-Pb isotopic data are presented in Table S2.

Zircon Hf isotope analyses

Zircon Hf isotope analyses were carried out using an ArF excimer laser ablation system, attached to a Neptune Plasma multi-collector ICP-MS, at FMS. A spot size of 50 μm was used for most analyses and the ablation spot for Hf analysis was sited at the same and/or near domain for the U-Pb dating. To monitor reliability and stability of the instrument, five standard zircon grains including GJ-1, 91500, Plešovice, Mud Tank, and Penglai were analyzed every ten to twelve unknown zircon spots. A mean $^{176}Hf/^{177}Hf$ ratio of 0.282010 ± 0.000003 (n = 30) was obtained for GJ-1, comparable with reference value of 0.282000 ± 0.000005 (Morel et al., 2008). Zircon standards 91500 and Plešovice gave mean $^{176}Hf/^{177}Hf$ ratios of 0.282304 ± 0.000003 (n = 24) and 0.282479 ± 0.000004 (n = 20), respectively, comparable to the recommended values of 0.282284 ± 0.000003 for 91500 (Wiedenbeck et al., 1995) and 0.282482 ± 0.000013 for Plešovice (Sláma et al., 2008). Measurements of Mud Tank and Penglai yielded mean ratios of 0.282510 ± 0.000003 (n = 22) and 0.282908 ± 0.000005 (n = 22), respectively, consistent with published values: 0.282497 ± 0.000018 for Mud Tank (Hawkesworth and Kemp, 2006) and 0.282906 ± 0.000010 for Penglai (Li et al., 2010). The Lu-Hf composition of the analyzed spots is presented in Table S6.

Mineral compositions

Mineral compositions were conducted at the Department of Earth Sciences, the University of HongKong, using a JEOL JXA-8230 electron microprobe. An accelerating voltage of 15 kV, a specimen current of 3.0×10^{-8} A and a beam size of 1 μm were employed. The analytical errors are generally less than 2%. All data were corrected using standard ZAF correction procedures and the detailed analytical procedures are similar to those described by Li and Zhuo. (2018). The mineral compositions are presented in Table S4.

Major and trace element analyses

Major and trace elements were analyzed at the ALS Chemex Company in Guangzhou. Major elements were obtained by X-ray fluorescence spectrometry (XRF) using fused lithium tetraborate glass pellets. Loss on ignition (LOI) values was measured using 1 g of powder heated to 1100℃ for 1 h. The accuracy of the analyses is within 1% for most major elements, which is determined on the Chinese National standard GSR-3. Trace elements, including rare earth elements (REE) were analyzed by inductively coupled plasma-mass spectrometry (ICP-MS). About 50 mg of powdered sample was placed in a steel-bomb with mixed HF + HNO_3 acid for 48 h in order to assure complete dissolution of the refractory minerals under high pressure. Analytical precision was generally better than 5 %. The major and trace element results are presented in Table S5.

Whole-rock Sr-Nd isotope analyses

The whole-rock Sr-Nd isotopic compositions were measured at the Guizhou Tuopu Resource and Environmental Analysis Center using the method of Qi et al. (2000). Chemical separation was undertaken by conventional ion-exchange techniques. Approximately 50 mg of powdered sample was placed in a PTFE bomb, after that 1ml of HF and 1 ml of HNO_3 were added. The sealed bombs were placed in an electric oven and heated to 185℃ for 36 h. After cooling, the bombs were heated on a hot plate to evaporate to dryness. 0.5ml HCl was added and evaporated to dryness. And then 4 ml of 1.5 MHCl was added. In order to dissolve the residue, the bomb was again sealed and placed in an electric oven at 125 ℃ for about 5 h. The solution was centrifuged at 4×10^3 rpm for 5min, and then the supernatant was loaded onto preconditioned Dowex 50 W×8 cm cation exchange resin columns for separation of sample matrix and Sr from Rb using 1.5 MHCl. LREE was eluted with 36 ml of 6 MHCl. The solution was evaporated to dryness and dissolved with 0.25×10^{-3} mol HCl. The resulting solution was loaded onto the pre-

conditioned Ln resin columns for separation of Nd from La, Ce, Pr, and Sm. A Neptune MC-ICP-MS was used to measure the $^{87}Sr/^{86}Sr$ and $^{143}Nd/^{144}Nd$ isotope ratios. NIST SRM-987 and JMC-Nd were used as certified reference standard solutions for $^{87}Sr/^{86}Sr$ and $^{143}Nd/^{144}Nd$ isotopes ratios, respectively. Analyses of NIST SRM-987 gave 0.710210 ± 0.000037 (2SD, n = 14) while the JMC Nd standard gave 0.511106 ± 0.000002 (2SD, n = 8). BCR-1 was used as the reference material. The Nd-Sr isotope compositions are presented in Table S7.

REFERENCES CITED

Hawkesworth, C. J., and Kemp, A. I. S., 2006, Using hafnium and oxygen isotopes in zircons to unravel the record of crustal evolution: Chemical Geology, v. 226, no. 3, p. 144-162, https://doi.org/10.1016/j.chemgeo.2005.09.018.

Jackson, S. E., Pearson, N. J., Griffin, W. L., and Belousova, E. A., 2004, The application of laser ablation-inductively coupled plasma-mass spectrometry to in situ U–Pb zircon geochronology: Chemical Geology, v. 211, no. 1, p. 47-69, https://doi.org/10.1016/j.chemgeo.2004.06.017.

Li, X.-C., and Zhou, M.-F., 2018, The nature and origin of hydrothermal REE mineralization in the Sin Quyen deposit, northwestern Vietnam: Economic Geology, v. 113, no. 3, p. 645-673.

Li, X. H., Long, W. G., Li, Q. L., Liu, Y., Zheng, Y. F., Yang, Y. H., Chamberlain, K. R., Wan, D. F., Guo, C. H., and Wang, X. C., 2010, Penglai zircon megacrysts: a potential new working reference material for microbeam determination of Hf–O isotopes and U–Pb age: Geostandards and Geoanalytical Research, v. 34, no. 2, p. 117-134, https://doi.org/10.1111/j.1751-908X.2010.00036.x.

Liu, Y., Hu, Z., Zong, K., Gao, C., Gao, S., Xu, J., and Chen, H., 2010, Reappraisement and refinement of zircon U-Pb isotope and trace element analyses by LA-ICP-MS: Chinese Science Bulletin, v. 55, no. 15, p. 1535-1546, https://doi.org/10.1007/s11434-010-3052-4.

Loiselet, C., Husson, L., and Braun, J., 2009, From longitudinal slab curvature to slab rheology: Geology, v. 37, no. 8, p. 747-750, https://doi.org/10.1130/g30052a.1.

Ludwig, K. R., 2012, User's manual for Isoplot version 3.75–4.15: a geochronological toolkit for Microsoft Excel: Berkeley Geochronology Center, Special Publication.

Morel, M. L. A., Nebel, O., Nebel-Jacobsen, Y. J., Miller, J. S., and Vroon, P. Z., 2008, Hafnium isotope characterization of the GJ-1 zircon reference material by solution and laser-ablation MC-ICPMS: Chemical Geology, v. 255, no. 1, p. 231-235, https://doi.org/10.1016/j.chemgeo.2008.06.040.

Qi, L., and Grégoire, D. C., 2000, Determination of Trace Elements in Twenty Six Chinese Geochemistry Reference Materials by Inductively Coupled Plasma-Mass Spectrometry: Geostandards Newsletter, v. 24, no. 1, p. 51-63, https://doi.org/10.1111/j.1751-908X.2000.tb00586.x.

Sláma, J., Košler, J., Condon, D. J., Crowley, J. L., Gerdes, A., Hanchar, J. M., Horstwood, M. S. A., Morris, G. A., Nasdala, L., Norberg, N., Schaltegger, U., Schoene, B., Tubrett, M. N., and Whitehouse, M. J., 2008, Plešovice zircon–A new natural reference material for U–Pb and Hf isotopic microanalysis: Chemical Geology, v. 249, no. 1–2, p. 1-35, http://dx.doi.org/10.1016/j.chemgeo.2007.11.005.

Wiedenbeck, M., Alle, P., Corfu, F., Griffin, W., Meier, M., Oberli, F., Quadt, A. v., Roddick, J., and Spiegel, W., 1995, Three natural zircon standards for U-Th-Pb, Lu-Hf, trace element and REE analyses: Geostandards newsletter, v. 19, no. 1, p. 1-23, https://doi.org/10.1111/j.1751-908X.1995.tb00147.x.

SUPPLEMENTAL FIGURES

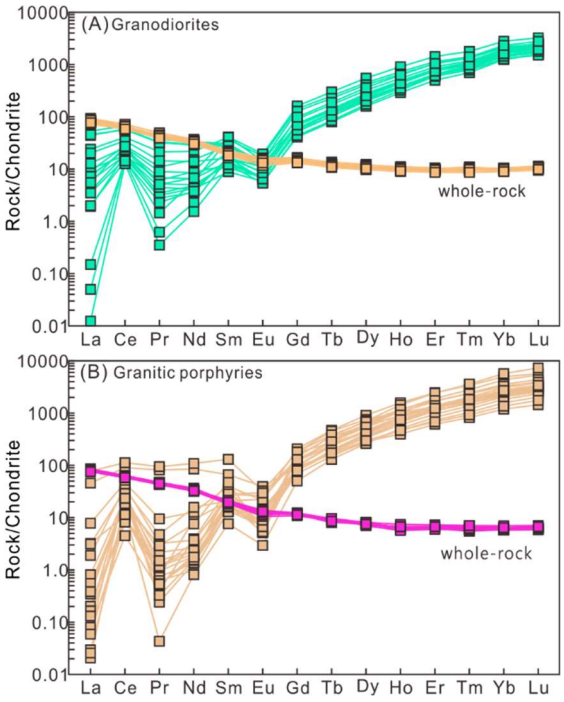

Fig. S1. REE patterns of analyzed zircon from the granitoids in Northern Yili Block.

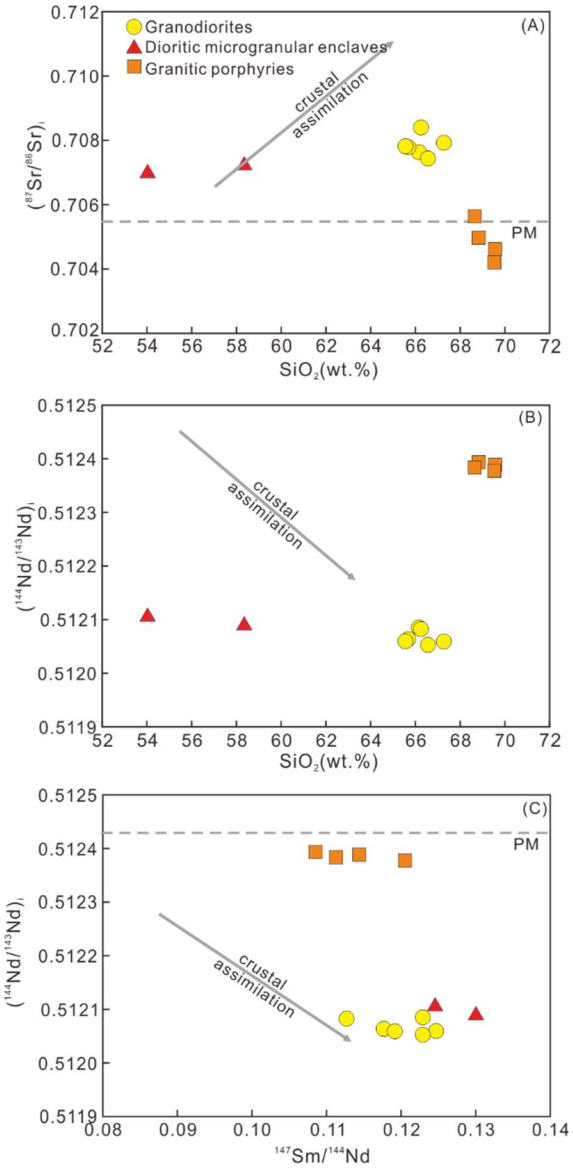

Fig. S2. (A) SiO_2 vs $(^{87}Sr/^{86}Sr)_i$; (B) SiO_2 vs$(^{143}Nd/^{144}Nd)_i$ and (C) $^{147}Sm/^{144}Nd$ vs $(^{143}Nd/^{144}Nd)_i$ diagrams for granitoids of the Northern Yili Block. See Table S5 for details.

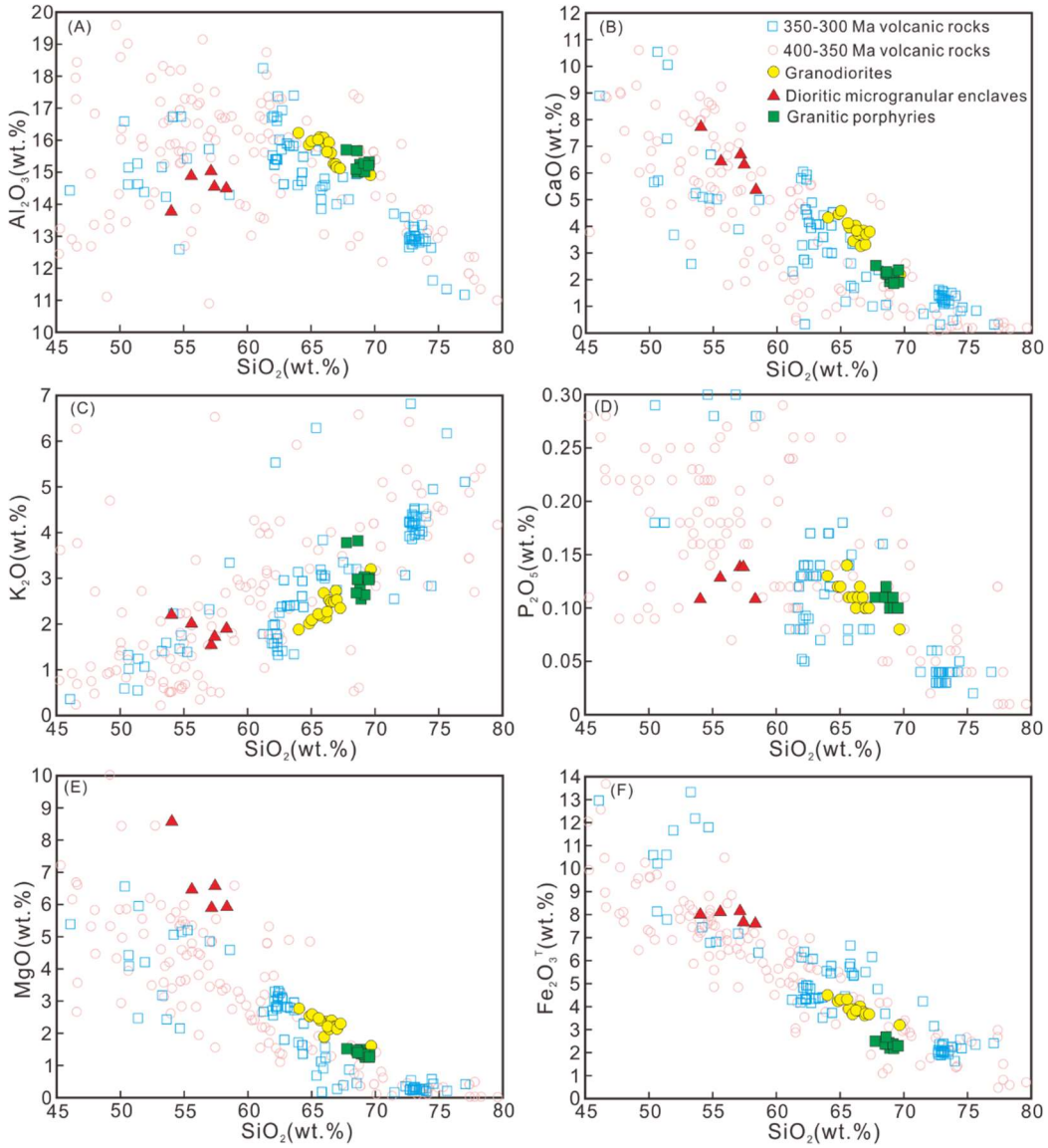

Fig. S3. Variation diagrams for major oxides versus SiO_2 for the magmatic rocks in the Northern Yili Block. See Tables S3 and S9 for details.